Mn^{2+} as a probe in $RbCaF_3$: local order parameter of the structural phase transition measured by ENDOR

1995 J. Phys.: Condens. Matter 7 8637

(http://iopscience.iop.org/0953-8984/7/45/019)

J. Phys.: Condens. Matter 7 (1995) 8637–8645. Printed in the UK

Mn^{2+} as a probe in $RbCaF_3$: local order parameter of the structural phase transition measured by ENDOR

F Lahoz†, P J Alonso†, R Alcalá†, T Pawlik‡ and J-M Spaeth‡

† Instituto de Ciencia de Materiales de Aragón, Universidad de Zaragoza, CSIC, Zaragoza, Spain

‡ Fachbereich Physik, Universität-GH, Paderborn, Germany

Received 26 June 1995

Abstract. The 195 K cubic-to-tetragonal structural phase transition (SPT) in $RbCaF_3$ crystals has been investigated by electron nuclear double resonance (ENDOR) using Mn^{2+} as a probe. The rotational angle of the fluorine octahedra, which is the local order parameter of the transition, has been determined at 40 K for the first and second shells of F^- ions surrounding the Mn^{2+} impurities. The values obtained are $5.1° \pm 0.2°$ for the first shell and $7.4° \pm 1°$ for the second shell. The thermal evolution of the first shell angle at temperatures close to that of the SPT has also been studied. The results have been compared with those in $RbCdF_3$:Mn^{2+}. The first shell angle measured at 40 K is similar to the one in $RbCdF_3$:Mn^{2+}. The second shell angle is almost double that in $RbCdF_3$:Mn^{2+}. Covalency effects through Cd^{2+} ions are suggested to account for this difference.

1. Introduction

Transition metal ions have been extensively used as local probes to study structural phase transitions (SPT) by magnetic resonance techniques. The high sensitivity of electron paramagnetic resonance (EPR) and electron nuclear double resonance (ENDOR) to the local environments of those ions allows the study of SPT even in cases where other techniques fail to detect them [1].

However, it is known that the probes influence the surrounding atoms in such a way that the local order parameter around the impurity does not coincide with that in the undoped crystal. This is most important in the case of EPR, where one usually gets information on the first coordination shell of the probe. ENDOR measurements provide information on further coordination shells whose behaviour with respect to the SPT is expected to be less influenced by the paramagnetic impurity.

In order to investigate the range of the perturbation due to the presence of the probe Studzinski and Spaeth [2] performed, some time ago, an ENDOR study of the SPT of $RbCdF_3$ using Mn^{2+} as a probe. At room temperature (RT) $RbCdF_3$ has a cubic perovskite structure where the Cd^{2+} ions are surrounded by an octahedron of fluorines as nearest neighbours and a cube of Rb^+ as next-nearest neighbours. Mn^{2+} enters these crystals in a Cd^{2+} site. At 124 K an SPT from cubic to tetragonal symmetry occurs. It consists of an elongation of the fluorine octahedra along one of the ⟨100⟩ axes together with an alternate rotation of the octahedra about the elongated axis. The rotation angle is the order parameter of the SPT [3, 4]. It was reported in [2] that not only the fluorines (FI) nearest to Mn^{2+} but even the second shell of fluorines (FII) around it are strongly influenced by the presence of the impurity in such a way that the local order parameter derived from the superhyperfine

0953-8984/95/458637+09$19.50

(SHF) interaction between the Mn^{2+} ion and the F II fluorines was about one half of that in the undoped crystal.

On the other hand, it has been found by Aoki and co-workers [5] that in some fluoroperovskites the SHF interaction between Mn^{2+} and the F II fluorines is much stronger when the divalent host cation has an outermost d shell than if the outer shell is of p type. This stronger interaction is associated with a bigger covalency between the impurity and the F II. The question arises whether this covalency also influences the order parameter experienced by the second shell of fluorines. It could be speculated that in a host crystal where the divalent cation does not have an outermost d shell, for example by replacing Cd in $RbCdFR_3$ by Ca, the reduced covalency to the second fluorine shell would increase the order parameter there. This could be measured as an increase of the rotation angle of the F II below the phase transition temperature. One would thus have an indication whether the reason for the reduced order parameters measured using Mn^{2+} as a probe in $RbCdF_3$ is caused simply by the lattice relaxation because of the misfit of the ionic radii or because of the influence of the covalent bonding between the probe and the nearest and next-nearest neighbours.

Because of this we have undertaken an ENDOR study of the SPT in $RbCaF_3$ using also Mn^{2+} as a probe. $RbCaF_3$ has the same crystal structure as $RbCdF_3$, a very similar lattice constant and the phase transition temperature from the cubic to the tetragonal phase is $T_c = 195$ K instead of 124 K for $RbCdF_3$. We present here the values of the order parameter derived from the SHF interaction parameters between Mn^{2+} and the fluorines of the first and second coordination shells. These results are discussed and compared with those in $RbCdF_3$.

2. Experimental set-up

Single crystals of $RbCaF_3$:Mn were grown by the Bridgmann method in a radio frequency (rf) heated furnace using vitreous carbon crucibles. Mn^{2+} was incorporated as MnF_2. The MnF_2 content in the starting materials ranged from 0.01% to 0.1%.

The stationary ENDOR measurements were performed with a computer-controlled X-band spectrometer (9.5 GHz) between 40 K and 300 K. Double ENDOR measurements [6] were performed in the same ENDOR set-up but using two radio frequencies f_1 and f_2; f_1 was set to a particular ENDOR line and its amplitude was modulated at 800 Hz while f_2 was swept through the range of interest and its amplitude was modulated at 5 Hz. Two lock-in amplifiers (800 Hz and 5 Hz) in series detected the double ENDOR signal.

3. Experimental results

From the previous study of Mn^{2+} in $RbCaF_3$ [7, 8] it was concluded that Mn^{2+} enters in a Ca^{2+} site.

ENDOR measurements have been performed at different temperatures between 200 K and 40 K. The EPR line which has been saturated to perform the ENDOR measurements corresponds to the $m_s = +1/2 \leftrightarrow m_s = -1/2$ electronic transition, with z component of nuclear magnetic moment $I_z = -1/2$ of ^{55}Mn ($I = 5/2$).

Figure 1 indicates the types of ^{19}F nuclei whose ENDOR signals have been detected. To describe the angular dependence of the ENDOR transitions we have used the following spin Hamiltonian (SH):

$$H = g\mu_B B_0 S + SAI + \tfrac{1}{2} b_2^0 O_2^0 - g_N \mu_N B_0 I + \sum_i SA_i I_i - \sum_i g_{N_F} \mu_N B_0 I_i \qquad (1)$$

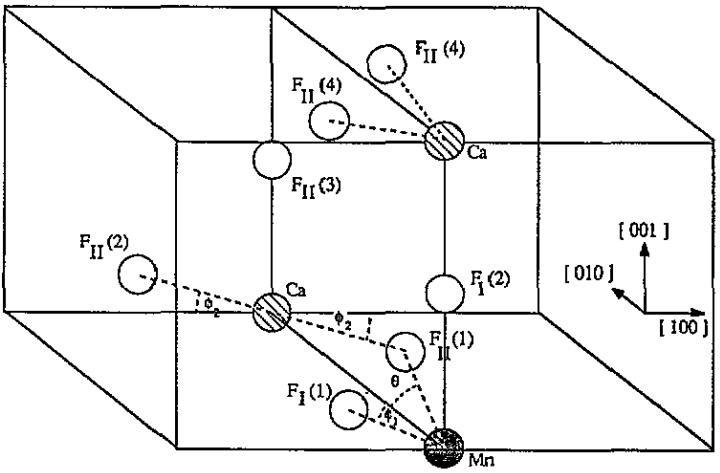

Figure 1. Neighbouring nuclei of the Mn^{2+} probe in the tetragonal phase of $RbCaF_3$, whose ENDOR spectra have been measured. The notation of the nuclei refers to table 1.

where the first term represents the electronic Zeeman effect, the second term expresses the hyperfine interaction (HF) with the ^{55}Mn nucleus, the third term introduces the second-order crystal field contributions, the fourth term gives the manganese nuclear Zeeman energy, the fifth term represents the SHF interaction with the neighbouring fluorines ($I(^{19}F) = 1/2$) and the last term gives the nuclear Zeeman interactions with these fluorines. The fourth-order crystal field term has been neglected because its contribution to the ENDOR transitions is very small and was below the resolution of our measurements. In (1) $S = 5/2$, $I = 5/2$ and $I_i = 1/2$. The orientation of the principal axes of the SHF tensors corresponding to each of the fluorines is given by the Euler angles θ, Φ and φ; θ is the angle between the z axis of the SHF tensor and the [010] direction for all the fluorines in the figure except for FI(2) and FII(4), for which θ is the angle between the z axis of the SHF tensor and the [001] direction.

The angular evolution of the ENDOR spectrum corresponding to the nearest-neighbour fluorines measured at 40 K with the magnetic field rotating in the (001) plane is shown in figure 2. Lines corresponding to different domains and different m_s values are observed. Only those lines corresponding to $m_s = -1/2$ will be analysed. Among them the most intense ones are those associated with the domains having the tetragonal axis perpendicular to the plane in which the magnetic field is rotated. These are the lines that we have used in our study. For a general direction of the applied magnetic field within the (001) plane five of these lines, some of them with a doublet structure, are observed. The doublet at about 31.2 MHz that does not show any angular dependence is due to FI(2). The other four lines are due to the fluorines in the (001) plane (FI(1)). Four lines instead of two are observed because of the two rotation directions of the fluorine octahedra.

The SHF parameters have been obtained from the least-squares fitting of the line positions calculated using (1) to the experimental ones. These SHF parameters are given in table 1. The isotropic and anisotropic SHF constants a and b, respectively, are related to the principal values of the usual SHF tensor **A**, which was found to be axial, by: $A_\perp = a - b$, $A_\parallel = a + 2b$. The small differences among the a and b values corresponding to FI(1) and FI(2) have been neglected.

It can also be seen in figure 2 that most of the lines show a doublet structure. To check

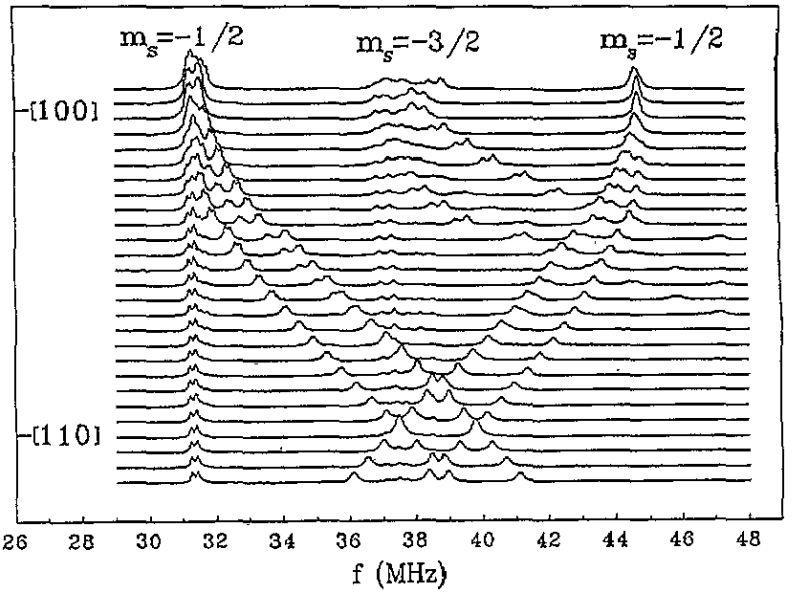

Figure 2. Angular dependence of the ENDOR lines of the $^{19}F^-$ nuclei nearest neighbours to Mn^{2+} measured in steps of 2° at 40 K. The applied magnetic field is rotated in a (001) plane. *Lines corresponding to* $m_s = -1/2$ *and* $m_s = -3/2$ *are observed.*

Table 1. SHF interaction parameters of two neighbour shells of Mn^{2+} in $RbCaF_3$. The SHF *constants a and b are given in MHz.* θ, Φ *and* φ *are the Euler angles (in degrees) of the* principal axis system of the SHF tensor as explained in the text.

	a	b	θ	Φ	φ
FI(1)	43.6(1)	9.2(1)	5.1(2)	0	0
FII(1)	0.000(5)	0.732(5)	28.4(5)	270	90
FII(2)	0.000(5)	0.549(5)	25.3(5)	270	90
FII(3, 4)	0.000(5)	0.646(5)	26.6(5)	270	90

for the origin of this structure, double ENDOR experiments have been performed. The results are given in figure 3, with the magnetic field at 25° from the [010] direction. The rf signal of frequency f_1 was applied in the different lines marked with an asterisk, while the frequency f_2 of the second rf signal was swept between 30 and 35 MHz and the double ENDOR effect was recorded. All the lines that appear in one spectrum have to be due to the same centre. Note that, for example, when setting f_1 to about 34.5 MHz only one of the FI(1) lines and the doublet of FI(2) are seen, while the FI(1) line due to the other rotated octahedra (f_1 at 32.5 MHz) is not seen (and *vice versa*). This proves that double ENDOR worked and that the doublet splitting cannot be associated with the presence of two slightly different centres.

The SHF interaction of the nearest fluorine shell as a function of temperature allows us to obtain some information about the structural phase transition (SPT) that takes place in these crystals [3, 4]. Because of this we have measured the thermal evolution of the ENDOR spectrum of FI nuclei. Our measurements have been taken similarly to those reported in [2].

The splitting of the ENDOR lines due to those nearest fluorines in the plane of rotation of

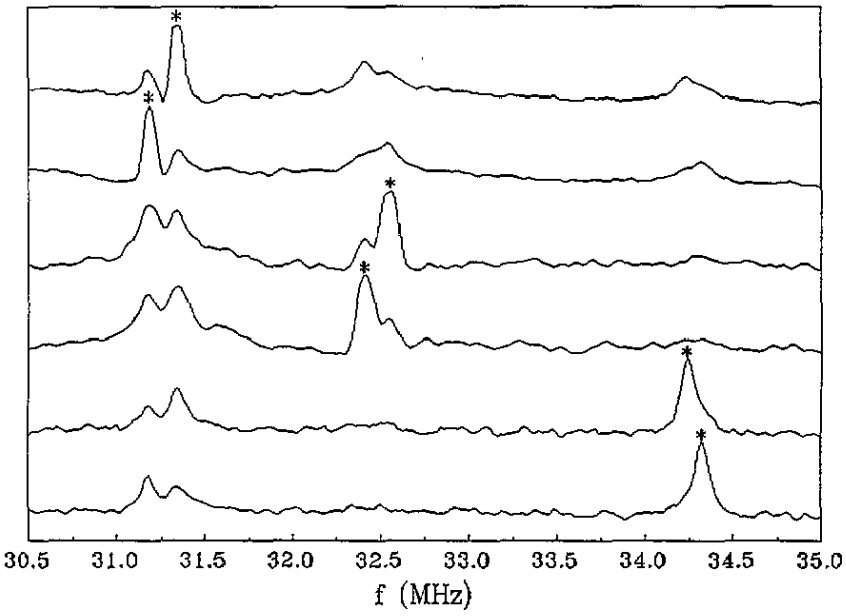

Figure 3. Double ENDOR measurements. The asterisk indicates the frequency, f_1, which has been fixed during each measurement.

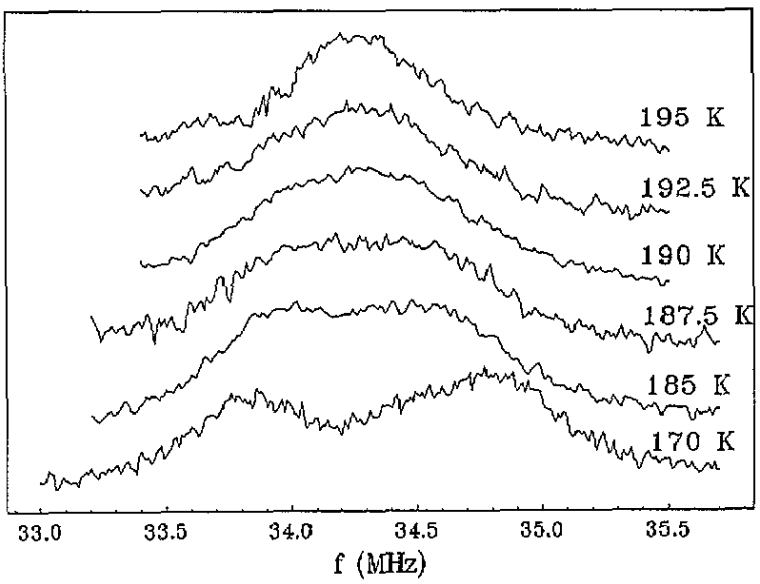

Figure 4. Splitting of the ENDOR signal of the F I(1) nucleus when the temperature is lowered from above T_c to below T_c. The external magnetic field was in the (001) plane at 25° to the [100] direction.

the magnetic field is proportional to the rotation angle of the F^- octahedra about the fourfold axis perpendicular to this plane. This splitting has been measured when the temperature is

lowered through the critical temperature (T_c) of the SPT. The results are shown in figure 4 for a magnetic field in the (001) plane and at 25° from the [100] direction. It can be seen that in the cubic phase ($T \geqslant 195$ K) the ENDOR line corresponding to FI(1) is a single one at about 34.2 MHz. When the temperature goes below T_c the alternate rotation of the fluorine octahedra results in different angles between the Mn–F bonding directions and the applied magnetic field. This produces the splitting of the ENDOR line shown in figure 4.

This splitting has been related to the rotation angle of the fluorine octahedra, that is the order parameter of the transition, using the line positions calculated with (1) and assuming that the z axis of the SHF tensor coincides with the Mn^{2+}–F^- direction. Thus, from the evolution of that splitting, the thermal evolution of the local order parameter has been determined. The results are given in figure 5. It can be seen that the order parameter increases with decreasing temperature. The inset in the figure gives a detailed view of the temperature region close to T_c together with the fitting to (2) (see below).

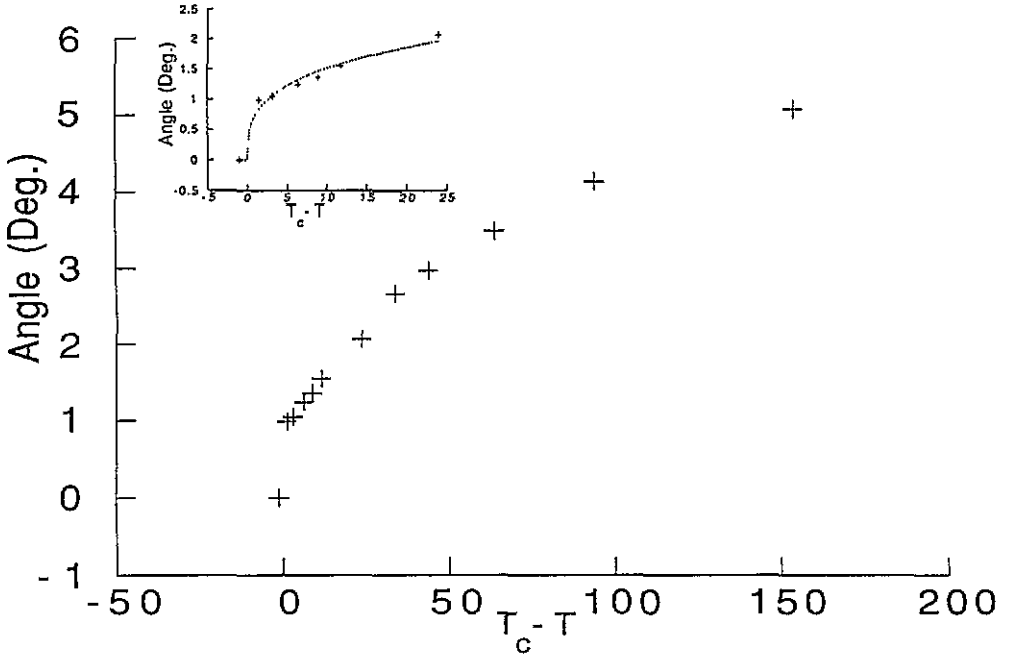

Figure 5. Temperature dependence of the local order parameter. The inset shows the behaviour in the proximity of T_c. The dotted curve represents the best fitting to an expression of the form $\phi = \phi_0 |T - T_c|^\beta$.

The ENDOR lines associated with the SHF interactions with the second shell of fluorines has also been measured at 40 K for the rotation of the static magnetic field in the (001) plane. The line positions are given in figure 6. The observation of so many ENDOR lines is again caused by the rotation of the FII octahedra below T_c as indicated in figure 1. The analysis of the angular dependence allowed the assignment of the different FII nuclei labelled as FII(1) to FII(4). In figure 6 some of these assignments are shown (see also section 4 below). The difference between the lines corresponding to FII(3) and FII(4) was below the resolution of our measurements (see below). The full curves in figure 6 are the calculated angular dependence using (1) assuming axial SHF tensors. The corresponding SHF parameters are given in table 1.

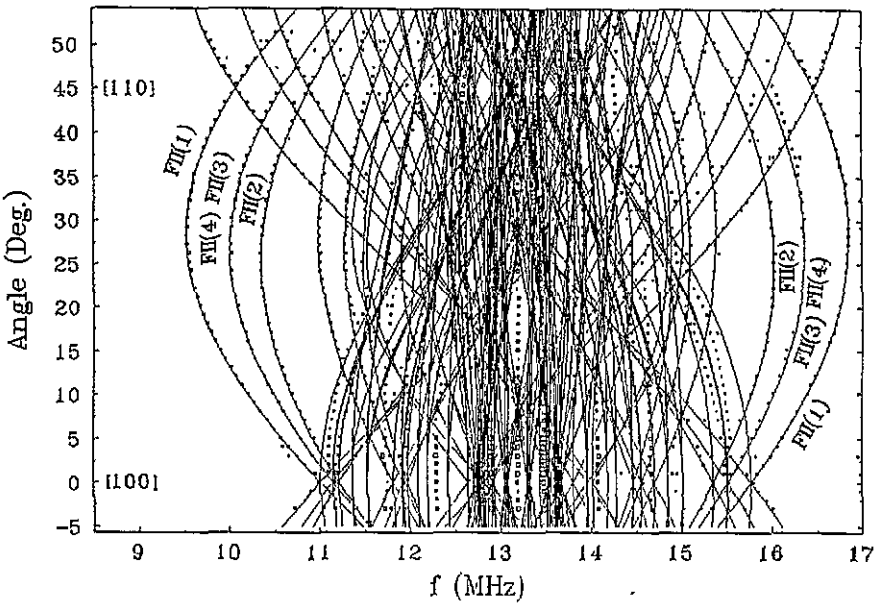

Figure 6. Angular dependence of the ENDOR signal associated with the next-nearest F^- neighbours measured at 40 K. The applied magnetic field was rotated in the (001) plane. Squares represent the measured transitions. The full curves give the angular dependence calculated with the SHF parameters of table 1. Some assignments of the ENDOR lines to the associated nuclei are indicated.

4. Discussion

The local order parameter ϕ for the nearest-neighbour fluorines is given by the θ angle of the SHF tensor. A value of $5.1° \pm 0.2°$ has been obtained (see table 1) when measured at 40 K. This value is smaller than the intrinsic angle of rotation, which has been found by neutron diffraction [3] to be 8°. This indicates a strong influence of the Mn^{2+} probe on the local order around it. Similar results have been obtained for the Mn^{2+} doped $RbCdF_3$ crystals [2], for which the local order parameter for the first fluorine shell is $4.7° \pm 0.1°$. The value of the isotropic SHF constant for the first fluorine shell for $RbCaF_3$:Mn is 43.6 MHz. The value previously obtained by EPR [7, 8] is very close to that.

With respect to the doublet structure observed in figure 2 it can be seen that for the lines due to the two equivalent FI(2) nuclei which are perpendicular to the plane of rotation of the external magnetic field (the doublet at the lowest frequencies in figure 2) the magnitude of the splitting is about 0.16 MHz. For the F nuclei that are in that plane of rotation the splitting is angular dependent. In a first-order calculation single lines instead of doublets are expected. On the other hand, the double ENDOR measurements indicate that the doublets are not due to different types of centre. However, because of the large SHF coupling, equivalent fluorine nuclei experience a pseudodipolar coupling and ENDOR lines of equivalent nuclei split [9]. These are always pairs of equivalent nuclei. The observed splittings can be explained quantitatively using the SHF parameters of table 1.

The critical temperature T_c which has been obtained from the results given in figures 4 and 5 is about 195 K, in good agreement with the T_c values measured by other techniques such as neutron or x-ray diffraction [3, 4].

The thermal evolution of the order parameter (figure 5) can be approximated in the

proximity of T_c by the equation

$$\phi = \phi_0 |T - T_c|^{\beta}. \tag{2}$$

The value estimated for the critical exponent is $\beta = 0.3(\pm 0.05)$. This result coincides, within experimental error, with the one obtained by other authors using different techniques [7, 10].

We will discuss now the results corresponding to the second shell of fluorines (F II). In order to assign the different parameters to each of the four different F II nuclei that appear in the tetragonal phase (see figure 1) we have used the following argument.

With the values of the crystallographic parameters for $RbCaF_3$ in the tetragonal phase [4] and with a local order parameter of 8° for this shell we have estimated the distances between the Mn^{2+} site and the different sites of the F II nuclei ($R(\mathrm{F\,II}(i))$). The values obtained are

$$R(\mathrm{F\,II}(1)) = 4.668\,\text{Å} \qquad R(\mathrm{F\,II}(2)) = 5.224\,\text{Å}$$
$$R(\mathrm{F\,II}(3)) = 4.954\,\text{Å} \qquad R(\mathrm{F\,II}(4)) = 4.994\,\text{Å}.$$

From the SHF parameters given in table 1 it can be seen that the isotropic part a is close to zero. Assuming that the overlap contribution to the anisotropic part b is negligible the z axis of the SHF interaction will be along the Mn–F bond direction and the b values will be given by the classical dipole–dipole interaction that decreases with R as $1/R^3$. Thus, looking at the three lines in the high- and low-frequency parts of the rotational diagram shown in figure 6, we have considered that the lowest b value that corresponds to the ENDOR angular evolution which is closer to the fluorine Larmor frequency (13.2 MHz) is associated with the largest Mn–F distance, i.e. with F II(2). The most external lines (highest b value) should be assigned to the smallest distance, i.e. to F II(1). The ENDOR line in between is due to the contributions of F II(3) and F II(4) which have very similar distances to the Mn^{2+} site and are not resolved in our measurements. This assignment is also in agreement with the values of θ given in table 1 that correspond to the angles between the [010] direction and the z axes of the SHF interaction tensors of the F II ions. It can be seen that the bigger value corresponds to F II(1) and the smaller one to F II(2).

This assignment differs from the one made [2] for $RbCdF_3$:Mn^{2+}, where F II(2) and F II(3) show a very close angular evolution. This difference may be understood because of the great influence of the Cd^{2+} ions on the second-fluorine-shell SHF interactions. The values of the isotropic part of the SHF interaction between Mn^{2+} and the F II fluorines is an order of magnitude smaller in $RbCaF_3$ than in $RbCdF_3$(2), in agreement with the findings of Aoki and co-workers [5] in $CsCaF_3$.

From the SHF constants given in table 1 the local order parameter of the SPT for the second fluorine shell has been estimated in two different ways. In both cases we have assumed as a first approximation that the relaxation of Ca^{2+} is negligible.

In the first method it has been considered that the anisotropic SHF constant is mainly due to the classical point dipole–dipole interaction. This is consistent with the low value obtained for the isotropic part a. In this approximation: $b = K/R^3$; K is given by $g\mu_B g_{N_F}\mu_N$, where g is the Mn^{2+} electronic g-factor and g_{N_F} is the $^{19}F^-$ nuclear g-factor. In our case we get the value $K = 74.41\,\text{MHz}\,\text{Å}^3$; R represents the Mn–F distance. From the R values it is straightforward to calculate the order parameter ϕ (see figure 1). The results obtained are $\phi_1 = 7.9° \pm 1°$ for F II(1) and $\phi_2 = 6.4° \pm 1°$ for F II(2) with a mean value of $\phi = 7.2° \pm 1°$.

In the second method we use the θ values given in table 1. Again a simple geometrical calculation allows us to obtain the ϕ values. The results are: $\phi_1 = 8.0° \pm 1°$ for F II(1) and $\phi_2 = 7.1° \pm 1°$ for F II(2). The mean value in this case is $\phi = 7.6° \pm 1°$.

It can be seen that the results obtained by the two methods are in good agreement. In both cases the rotation angle obtained for F II(1) is smaller than the one obtained for F II(2). This may be due to a small inwards relaxation of the Ca and F II ions.

The intrinsic order parameter measured by neutron diffraction [4] is 8°. This value is very close to those obtained for the second fluorine shell. It indicates that the influence of the lattice distortion around the impurity on the rotational angle of the second shell of fluorines is small for $RbCaF_3$. This result is markedly different from the one obtained in [2] for $RbCdF_3$:Mn using similar procedures. In this case the rotation angle estimated for the second shell of fluorines was about 4°.

From our results we can conclude that the influence of Mn^{2+} on the first fluorine shell is comparable in both $RbCdF_3$ and $RbCaF_3$ crystals. From the a values an inwards relaxation of the first shell of fluorines has been estimated by Barriuso and Moreno [11] in both cases with a Mn–F I distance slightly smaller in the Cd compound than in the Ca one. The local order parameter associated with these F I ions is similar in both compounds but significantly smaller than that of the undoped crystal.

On the other hand, we can also conclude that the influence of Mn^{2+} on the rotation of the second shell of fluorines is small in the case of $RbCaF_3$. The local order parameter associated with these F II ions is close to that in the undoped crystals. This is at variance with the behaviour found in $RbCdF_3$. The reason for this difference may be the significant covalent interaction between Mn^{2+} and F II ions in the Cd^{2+} containing compounds which must be due to a transferred SHF interaction through the Cd^{2+} ions.

Acknowledgments

This work has been supported by the CICYT (Spain) under project MAT-92-1279. Financial support of the Stiftung Volkswagenwerk and the Spanish–German Cooperation Committee is also aknowledged.

References

[1] Owens F J 1979 *Magnetic Resonance of Phase Transitions* ed F J Owens, C P Poole and M A Farach (New York: Academic)
[2] Studzinski P and Spaeth J M 1986 *J. Phys. C: Solid State Phys.* **19** 6441
[3] Bates J B, Mayor R W and Modine F A 1975 *Solid State Commun.* **17** 1347
[4] Bulou A, Ridou C, Rousseau M and Nouet J 1980 *J. Physique* **41** 87
[5] Aoki H, Arakawa M and Yosida T 1983 *J. Phys. Soc. Japan* **52** 2216
[6] Spaeth J M, Niklas J K and Bartram R H 1992 *Structural Analysis of Point Defects in Solids (Springer Series in Solid-State Science 43)* (Berlin: Springer)
[7] Rousseau J J, Rousseau M and Fayet J C 1976 *Phys. Status Solidi* b **73** 625
[8] Lahoz F, Alonso P J, Villacampa B and Alcalá R 1995 *Radiat. Eff. Defects Solids* **133** at press
[9] Feuchtwang T E 1962 *Phys. Rev.* **126** 1628
[10] Villacampa B, Alcalá R, Alonso P J and Spaeth J M 1993 *J. Phys.: Condens. Matter* **5** 747
[11] Barriuso M J and Moreno M 1983 *Phys. Rev.* B **29** 3623